Molecular Crystals and Liquid Crystals

Publication details, including instructions for authors and subscription information:
http://www.tandfonline.com/loi/gmcl20

Determination of Material Constants of Antiferroelectric Liquid Crystal Mixture CS4001

Lesley A. Parry-Jones [a], Emmanouil E. Kriezis [a] & Steve J. Elston [a]

[a] Department of Engineering Science, Oxford University, Oxford, United Kingdom

Version of record first published: 18 Oct 2010

To cite this article: Lesley A. Parry-Jones, Emmanouil E. Kriezis & Steve J. Elston (2004): Determination of Material Constants of Antiferroelectric Liquid Crystal Mixture CS4001, Molecular Crystals and Liquid Crystals, 410:1, 129-140

To link to this article: http://dx.doi.org/10.1080/15421400490436205

Mol. Cryst. Liq. Cryst., Vol. 410, pp. 129/[657]–140/[668], 2004

ISSN: 1542-1406 print/1563-5287 online
DOI: 10.1080/15421400490436205

DETERMINATION OF MATERIAL CONSTANTS OF ANTIFERROELECTRIC LIQUID CRYSTAL MIXTURE CS4001

Lesley A. Parry-Jones, Emmanouil E. Kriezis, and Steve J. Elston
Department of Engineering Science, Oxford University, Parks Road, Oxford, OX1 3PJ, United Kingdom

This work outlines a number of experimental techniques that can be used to determine some fundamental material constants in antiferroelectric liquid crystal materials, exemplified by results for the commercial AFLC mixture CS4001. The parameters measured range from the helical pitch of the material to the interlayer interaction coefficients, elastic constants and viscosities. The experimental methods employed include a variety of both optical and dielectric techniques.

Keywords: antiferroelectric; dielectric; elastic constant; interlayer interaction; liquid crystal; pitch; time constant; viscosity

INTRODUCTION

In predicting the behaviour of liquid crystals under applied electric fields, it is necessary not only to understand the physical mechanisms behind the liquid crystal molecular response, but also to have values for the material parameters, for example the viscosity and elastic constants. In this work, a number of experimental techniques are presented, which have been used to provide room temperature measurements of some important material parameters of the commercial antiferroelectric liquid crystal mixture, CS4001 from Chisso. The experimental methods used include a variety of dielectric and optical techniques, and were performed on both homeotropic and planar aligned devices of a range of thicknesses.

The authors would like to acknowledge the financial support of the EPSRC and the provision of a CASE award and test cells by Sharp Laboratories of Europe, Oxford.

Address correspondence to Lesley A. Parry-Jones, Department of Engineering Science, Oxford University, Parks Road, Oxford, OX1 3PJ, United Kingdom.

PITCH

In order to measure the pitch of an AFLC, a thick, planar aligned device is made, so that the bulk of the cell has a helical structure. The mismatch between the bulk helical structure and the non-helical structure at the surfaces causes line defects (or dechiralisation lines) to form near both surfaces of the device. The lines run parallel to the smectic layers, perpendicular to the helical axis, and in an AFLC material are separated by one half of the pitch of the material. The separation of the lines in CS4001 is measured to be 1.4 μm and therefore the pitch p of material is:

$$p = 2.8\,\mu\text{m} \tag{1}$$

TIME CONSTANTS

Two of the collective modes of an AFLC are goldstone modes in which the motion of the directors around the smectic cone in adjacent layers are either in the same direction (the in-phase mode) or in opposite directions (the anti-phase mode) [1,2]. These modes each have an associated time constant that can be measured either dielectrically or optically. It is well known that the anti-phase mode has a much smaller time constant than the in-phase mode [1].

Dielectric Method

To measure the time constants dielectrically, a planar aligned device is connected to an impedance analyser, which probes the device with a small ac electric field. The real and imaginary parts of the device impedance are measured as a function of the signal frequency, and from these the real and imaginary parts of the dielectric permittivity of the material can be calculated. The result is known as a dielectric spectrum, and is shown for a thick (helical) sample of CS4001 in Figure 1. As the frequency of the probing field is increased, the real part of the permittivity goes through a series of downward steps, each step at the relaxation frequency a dielectric mode. At these frequencies, the imaginary part of the dielectric constant goes through a peak, indicating the loss that occurs as the mode relaxes out. The in-phase and anti-phase mode relaxations occur at (100 ± 10) Hz and (20 ± 5) kHz, respectively. We therefore have the following time constants:

$$\begin{aligned} \tau_{in\text{-}phase(helical)} &= (1.6 \pm 0.1)\,\text{ms}, \\ \tau_{anti\text{-}phase(helical)} &= (8.0 \pm 2.0)\,\mu\text{s}, \end{aligned} \tag{2}$$

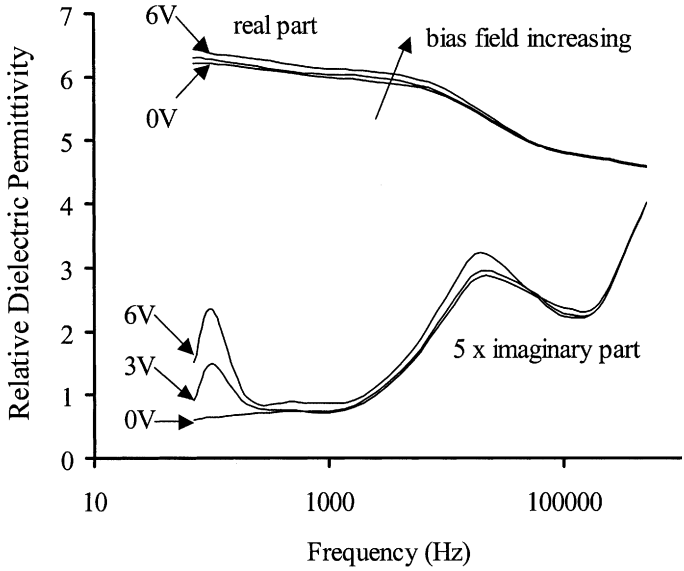

FIGURE 1 Measured dielectric spectrum of a thick (helical) planar aligned sample of CS4001. There are two collective Goldstone modes at frequencies of about 100 Hz and 20 kHz, characterised by a step down in the real part of the dielectric constant and a peak in the imaginary part. These give the time constants of the in-phase and anti-phase modes respectively.

for the sample of CS4001 used to obtain the experimental results in Figure 1.

Optical Method

The time constants can also be measured optically, as illustrated in Figure 2, this time for a thin (surface stabilised) planar aligned CS4001 device. The diagram shows the optical response of the device, between crossed polarisers, to an applied pulse, and the relaxation that occurs after the voltage is removed. It is clear that the relaxation occurs through a two-stage process, the two stages having very different relaxation times. The first process corresponds to the anti-phase mode, and the second to the in-phase mode. The time constants are measured to be of the order:

$$\begin{aligned} \tau_{in\text{-}phase} &= (0.5 \pm 0.1)\,\text{ms}, \\ \tau_{anti\text{-}phase} &= (7.0 \pm 1.0)\,\mu\text{s}, \end{aligned} \tag{3}$$

for a 1 μm cell of CS4001. In order to compare these time constants with those measured in the helical device, we refer to the results of Refs. [3]

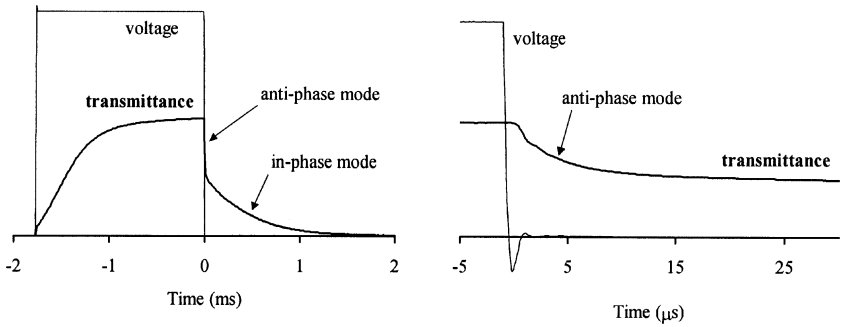

FIGURE 2 The time constants of the collective modes can also be measured optically, as illustrated here. The relaxation of the AFLC after the voltage pulse is removed clearly shows a fast decay followed by a slower one: these correspond to the anti-phase and in-phase modes, respectively.

and [4], which present expressions for the time constants $\tau_{in\text{-}phase}$ and $\tau_{anti\text{-}phase}$ in terms of other material parameters for both helical and surface stabilised devices:

$$\begin{aligned} \tau_{in\text{-}phase(helical)} &= \frac{\eta_{in\text{-}phase}\, p^2}{16\pi^2 K_x}, \tau_{anti\text{-}phase(helical)} = \frac{\eta_{anti\text{-}phase}}{2(\Gamma + 4\Delta)}, \\ \tau_{in\text{-}phase(surf.stab.)} &= \frac{\eta_{in\text{-}phase} d^2}{\pi^2 K_z}, \tau_{anti\text{-}phase(surf.stab.)} = \frac{\eta_{anti\text{-}phase}}{2(\Gamma + 4\Delta)}, \end{aligned} \tag{4}$$

where $\eta_{in\text{-}phase}$ and $\eta_{anti\text{-}phase}$ are the viscosities of the in-phase and anti-phase modes, d is the cell thickness, and K_x and K_z are the interlayer and intralayer elastic constants, respectively. Γ and Δ are coefficients of the interlayer coupling energy, and are discussed in the next section. It is clear that the anti-phase mode time constant should be independent of whether the helical structure is present or not. This is seen in the experimental results, i.e., 8 μs and 7 μs for thick and thin devices, respectively. However, the in-phase mode time constant clearly depends on the device geometry and the elastic constants involved, and therefore cannot be compared without further information. This point will be returned to later in this paper.

INTERLAYER COUPLING COEFFICIENTS

Dielectric Method

In modelling AFLCs, an interlayer interaction energy of the form:

$$F = \Gamma \cos^2 \phi_b - \Delta \cos^2 2\phi_b \tag{5}$$

is often assumed [5,6]. The first term is a dipolar term that favours anticlinic ordering in preference to synclinic ordering (when Γ is positive). The second term is a quadrupolar term which favours both AF and F states equally (Δ is also positive). It is possible to measure values for the coefficients Γ and Δ using a variety of experimental techniques. For example, the strength of the anti-phase relaxation in the dielectric spectrum should be [6,7]:

$$\Delta\varepsilon = \frac{P_s^2}{4\varepsilon_0(\Gamma + 4\Delta)} \tag{6}$$

which, knowing the spontaneous polarisation P_s, should give a value for the combination of parameters: $\Gamma + 4\Delta$. In the case of CS4001, where:

$$P_s = 79.7\,\mathrm{nC/cm^2} \qquad \text{(from Chisso)}, \tag{7}$$

and $\Delta\varepsilon \sim 1$, we obtain:

$$\Gamma + 4\Delta \sim 1.8 \times 10^4\,\mathrm{J/m^3}. \tag{8}$$

A more accurate value can be obtained by measuring the low frequency (1 kHz) dielectric constant as a function of applied field, as shown in Figure 3 for a helical sample of CS4001. It can be seen that the dielectric constant first increases with field as the helix unwinds, and then decreases at it switches into the ferroelectric state. According to Ref. [7], the difference in dielectric constant between the helical AF state and both the unwound AF state and ferroelectric states is also given by Eq. (6) above. Since this is measured to be $\Delta\varepsilon = (1.13 \pm 0.15)$, we obtain a more accurate value:

$$\Gamma + 4\Delta = (1.6 \pm 0.2) \times 10^4\,\mathrm{J/m^3}. \tag{9}$$

As well as determining $\Gamma + 4\Delta$ dielectrically, it can also be measured optically using a conoscopic technique.

Conoscopic Method

In order to determine further physical parameters in CS4001, the conoscopic image of a thick ($\sim$50 μm) homeotropically aligned device with in-plane electrodes was compared with the predictions of an optics modelling program based on an extension [8] of the Jones matrix method [9] to allow for oblique incidence of light. The experimental arrangement for the measurements and the theoretical model used to generate the director structure for the input to the optics program have been reported elsewhere [10].

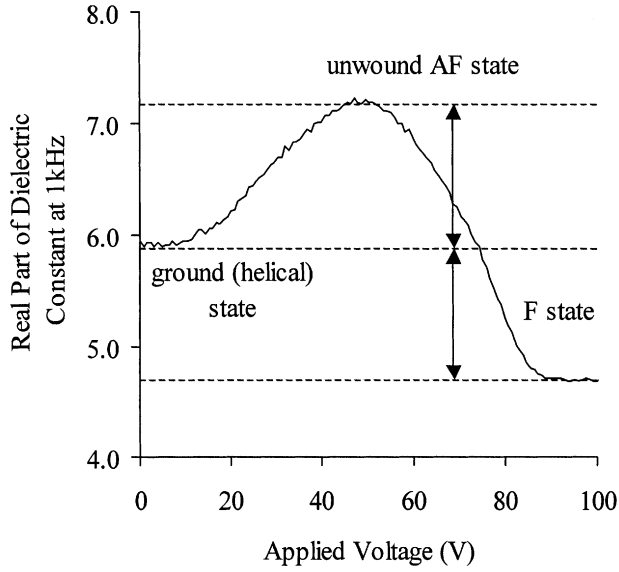

FIGURE 3 Experimental results for the low frequency (1 kHz) dielectric constant of a thick (helical) planar aligned sample of CS4001, as a function of applied bias field. Note that the dielectric permittivity of the helical AF state (0 V) is exactly midway between those of the unwound AF (about 50 V) and ferroelectric (above 90 V) states. The changes in perimittivity can be used to calculate the parameter $\Gamma + 4\Delta$.

The conoscopic image recorded experimentally for the ground state of the cell is as shown in Figure 4(a), and compares very well with the predicted conoscopic image for an undistorted helical structure, as shown in Figure 4(b). Both images are typical of a uniaxial structure with its axis aligned along the symmetry axis of the optical arrangement. When an electric field is applied to the liquid crystal via the in-plane electrodes, the helical structure distorts and becomes biaxial, with a small shift in the centre of the conoscopic image. The theoretical model shows [10] that the helix distortion is controlled by the dimensionless parameter:

$$X = \frac{E^2 P_s^2 p^2}{4K(\Gamma + 4\Delta)}. \tag{10}$$

The best fit between experiment and theory (Figs. 4(c) and 4(d) respectively) was for $X = 12.7 \pm 1.6$. With $p = 2.8\,\mu m$ and $P_s = 79.7\,nC/cm^2$, and the fact that the experimental data was taken for an 800 V potential difference across a 1 mm gap, we therefore have:

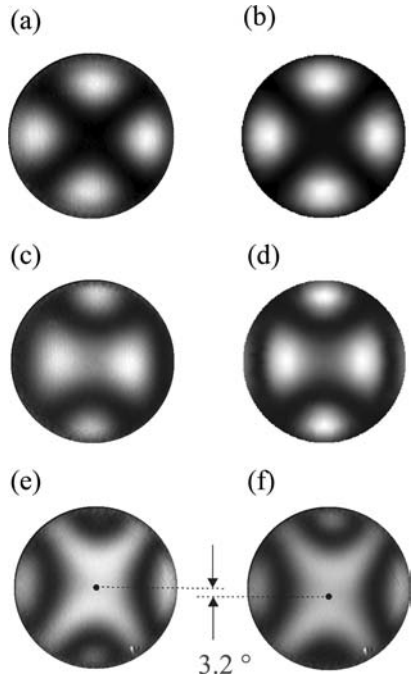

FIGURE 4 A comparison of experimental and theoretical conoscopic plots can be used to determine some interlayer parameters. Parts (a) and (b) compare the experimental and theoretical ground states, which have uniaxial symmetry. Under moderate applied field (<1V/μm), the helical structure is distorted but not unwound. As shown by the experimental and theoretical results in parts (c) and (d), this results in biaxial symmetry. Parts (e) and (f) show experimental results for higher fields (±2 V/μm) in which the helical structure is unwound. Note that the shift in the centre of the conoscopic image (the pretransitional effect) is visible at these high fields.

$$K_x(\Gamma + 4\Delta) = (2.56 \pm 0.32) \times 10^{-8}\,\mathrm{J^2/m^4}. \tag{11}$$

Above a critical field, the helical structure unwinds, and the shift in the centre of the conoscopic image becomes more pronounced, as illustrated in Figures 4(e) and (f), for the cases of applied voltages of ±2000 V (across a 1 mm gap). The lack of a helical structure means that now the results of the theoretical model are controlled by the parameter:

$$Y = \frac{EP_s}{2(\Gamma + 4\Delta)}. \tag{12}$$

The shift in the centres of the experimentally measured conoscopic images is $\pm 1.6^{\circ}$, which is also achieved in the theoretical predictions for $Y = (3.4 \pm 0.4) \times 10^{-2}$. Combining this result with Eqs. (11) and (12) leads to:

$$\begin{aligned} \Gamma + 4\Delta &= (1.5 \pm 0.2) \times 10^4 \,\mathrm{J/m^3}, \\ K_x &= (1.7 \pm 0.4) \times 10^{-12} \,\mathrm{N}. \end{aligned} \tag{13}$$

Decoupling Γ and Δ

In order to determine Γ and Δ separately, rather than as the combination $\Gamma + 4\Delta$, the holding voltage of the AFLC can be measured. This is the voltage at which the AF and F states are of equal energy, and therefore a mixed state of AF and F domains does not change with time. It can be measured by switching the device into a multi-domain state, and then finding the voltage at which the transmission of the device remains constant. In a 9.5 μm device of CS4001 it was measured to be (56 ± 2)V at room temperature. According to our theoretical model [6], the AF and F states are equal in energy when:

$$E = \frac{(1 + c)(\Gamma - 4c^2\Delta)}{P_s}, \tag{14}$$

where c is the solution to:

$$4\Delta(3c - 4)c^3 - (\Gamma + 4\Delta)(c - 2)c - \Gamma = 0. \tag{15}$$

Using these equations simultaneously with $\Gamma + 4\Delta = (1.6 \pm 0.2) \times 10^4 \,\mathrm{J/m^3}$ leads to:

$$\begin{aligned} \Gamma &= (4.4 \pm 0.5) \times 10^3 \,\mathrm{J/m^3}, \\ \Delta &= (2.9 \pm 0.4) \times 10^3 \,\mathrm{J/m^3}. \end{aligned} \tag{160}$$

ELASTIC CONSTANTS

As discussed above, the comparison of conoscopic measurements and theoretical predictions leads to a value for the interlayer elastic constant $K_x = (1.7 \pm 0.4) \times 10^{-12}$ N (Eq. (13)). A value for the *intra*layer elastic constant can be obtained by measuring the Freedericksz voltage in a surface stabilised device (see Fig. 5). As realised by Zhang *et al.* [11], the

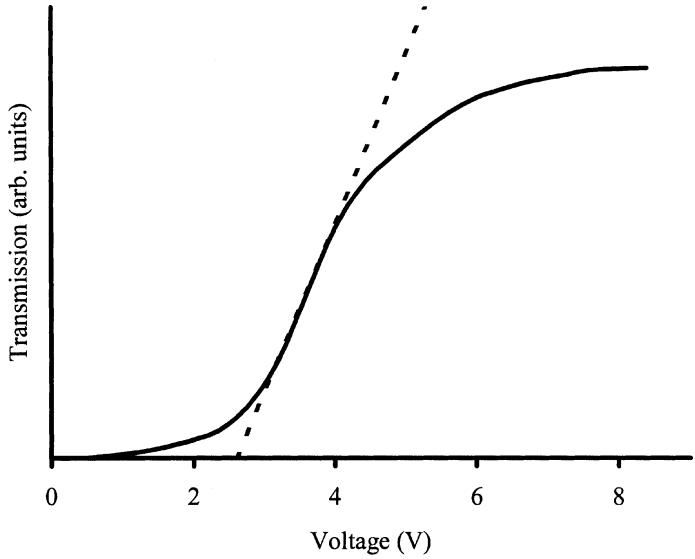

FIGURE 5 Optical transmission of a surface stabilised AFLC device between crossed polarisers as a function of applied field. The onset of transmission is characterised by a distinct threshold or Freedericksz voltage.

switching of a surface stabilised AFLC is analogous to that of a nematic, and therefore exhibits a voltage threshold:

$$V_{Freedericksz} = \frac{\pi\sqrt{2K_z(\Gamma + 4\Delta)}}{P_s} \tag{17}$$

Knowing P_s and $\Gamma + 4\Delta$, a measurement of the Freedericksz voltage therefore allows K_z to be determined. In CS4001, $V_{Freedericksz} = (2.6 \pm 0.1)\,\mathrm{V}$, therefore:

$$K_z = (1.4 \pm 0.3) \times 10^{-11}\,\mathrm{N}. \tag{18}$$

Note the fact that the interlayer and intralayer elastic constants are almost an order of magnitude different, i.e. the elastic constant is highly anisotropic. This has implications in determining the critical pitch to thickness ratio for surface stabilisation of the helical superstructure in AFLCs, since the critical parameter is:

$$\frac{p}{d}\sqrt{\frac{K_z}{K_x}}. \tag{19}$$

TABLE 1 A Summary of the Room Temperature Constants Measured, Methods Used and Values Obtained in this Work

Parameter	What is it?	Method	Value
p	helical pitch	dechiralisation line separation (microscope)	2.8 μm
$\tau_{in\text{-}phase(helical)}$	time constant of in-phase collective mode in helical device	dielectric spectrum	(1.6 ± 0.2) ms
$\tau_{anti\text{-}phase(helical)}$	time constant of anti-phase collective mode in helical device	dielectric spectrum	(8.0 ± 2.0) μs
$\tau_{in\text{-}phase(surf.stab.)}$	time constant of in-phase collective mode in surface stabilised device	optical relaxation	(0.5 ± 0.1) ms (1 μm device)
$\tau_{anti\text{-}phase(surf.stab.)}$	time constant of anti-phase collective mode in surface stabilised device	optical relaxation	(7.0 ± 1.0) μs
$\Gamma + 4\Delta$	combination of dipolar and quadrupolar interlayer coupling coefficients	dielectric 1 dielectric 2 conoscopic	~ 1.8 1.6 ± 0.2 1.5 ± 0.2 $(\times 10^4\,\mathrm{J/m^3})$
Γ	dipolar interlayer coupling coefficient	holding voltage	(4.4 ± 0.5) $\mathrm{J/m^3}$
Δ	quadrupolar interlayer coupling coefficient	holding voltage	(2.9 ± 0.4) $\mathrm{J/m^3}$
K_x	interlayer elastic constant	conoscopy	(1.7 ± 0.4) $\times 10^{-12}$N
K_z	intralayer elastic constant	Freedericksz voltage	(1.4 ± 0.3) $\times 10^{-11}$ N
$\eta_{in\text{-}phase}$	viscosity for in-phase collective mode	dielectric optical	0.054 ± 0.019 0.069 ± 0.028 Pa s
$\eta_{anti\text{-}phase}$	viscosity for anti-phase collective mode	dielectric optical	0.26 ± 0.06 0.22 ± 0.06 Pa s

VISCOSITIES

Now that the parameter $\Gamma + 4\Delta$, and the elastic constants K_x and K_z are known, the viscosities can be calculated using Eq. (4). Let us consider firstly the viscosity of the anti-phase motion, $\eta_{anti\text{-}phase}$. It was noted above that the time constant was independent of the cell thickness. Therefore we

use the average time constant, $\tau_{anti-phase} = (7.5 \pm 1.0)\,\mu s$, and $\Gamma + 4\Delta = (1.6 \pm 0.2) \times 10^4\,J/m^3$ to calculate:

$$\eta_{anti\text{-}phase} = (0.24 \pm 0.06) Pa\,s. \tag{20}$$

We can compare the time constants of the in-phase modes in helical and surface stabilised devices by calculating the in-phase viscosity for both, using Eq. (4), and comparing the two. For the helical device, we use Eqs. (1), (2), (4) and (13) to calculate:

$$\eta_{in\text{-}phase} = (0.054 \pm 0.019) Pa\,s. \tag{21}$$

For the surface stabilised device, we use Eqs. (3), (4) and (18), and the fact that the device is 1 μm thick to calculate:

$$\eta_{in\text{-}phase} = (0.069 \pm 0.028) Pa\,s, \tag{22}$$

which agrees well with Eq. (21).

CONCLUSIONS

In this paper, we have presented experimental methods for determining some important material parameters in antiferroelectric liquid crystals. The methods have involved a number of different optical and dielectric techniques. The results obtained at room temperature for the commercial AFLC mixture are summarised in Table 1.

REFERENCES

[1] Buivydas, M., Gouda, F., Lagerwall, S., & Stebler, B. (1995). The molecular aspect of the double absorption peak in the dielectric spectrum of the antiferroelectric liquid crystal phase. *Liq. Cryst.*, *18*(6), 879–886.

[2] Panarin, Y., Kalinovskaya, O., & Vij, J. (1998). The investigation of the relaxation processes in antiferroelectric liquid crystals by broad band dielectric and electro-optic spectroscopy. *Liq. Cryst.*, *25*(2), 241–252.

[3] Parry-Jones, L. (2001). *Field Driven Helix Distortion and Switching in Antiferroelectric Liquid Crystals*. DPhil Thesis, Oxford University, United Kingdom.

[4] Parry-Jones, L. & Elston, S. (2002). Theoretical prediction of the dielectric spectrum of an antiferroelectric liquid crystal. *J. Appl. Phys.*, *92*(1), 449–455.

[5] Qian, T. & Taylor, P. (1999). Field-induced phase transitions in antiferroelectric liquid crystals. *Phys. Rev., E 60*(3), 2978–2984.

[6] Parry-Jones, L. & Elston, S. (2001). Importance of quadrupolar ordering in antiferroelectric liquid crystal devices. *Appl. Phys. Lett.*, *79*(13), 2097–2099.

[7] Parry-Jones, L. & Elston, S. (2001). Field-driven helix unwinding in antiferroelectric liquid crystals. *Phys. Rev., E 63*, 050701(R).

[8] Gu, C. & Yeh, P. (1999). Extended Jones matrix method and its application in the analysis of compensators for liquid crystal displays. *Disp.*, *20*, 237–257.

[9] Jones, R. (1941). A new calculus for the treatment of optical systems. *J. Opt. Soc. Am.*, *62*, 488–493.
[10] Parry-Jones, L., Kriezis, E., & Elston, S. (2002). Conoscopic observations of a homeotropically aligned antiferroelectric liquid crystal device: a comparison of theory and experiment. *Jap. J. Appl. Phys.*, *41*, L1485–L1487.
[11] Zhang, S., Wen, B., Keast, S., Neubert, M., Taylor, P., & Rosenblatt, C. (2000). Freedericksz transition in an anticlinic liquid crystal. *Phys. Rev. Lett.*, *4*(18), 4140–4143.